J Mater Sci (2009) 44:4040–4046
DOI 10.1007/s10853-009-3564-y

Growth and characterization of bamboo-like multiwalled carbon nanotubes over Cu/Al_2O_3 catalyst

Bin Xue · Run Liu · Wan-Zhen Huang · Yi-Fan Zheng · Zhu-De Xu

Received: 16 January 2009 / Accepted: 12 May 2009 / Published online: 26 May 2009

Abstract The growth of bamboo-like multiwalled carbon nanotubes (MWCNTs) over Cu/Al_2O_3 catalyst by chemical vapor deposition under atmospheric pressure using ethanol as the carbon source has been demonstrated. The obtained MWCNTs are dominant with bamboo-like morphology. The morphologies, graphitization degree, and microstructures of the products were characterized by transmission electron microscopy, X-ray diffraction, Raman spectroscopy, field emission scanning electron microscopy, high-resolution transmission electron microscopy, and selected area electron diffraction. The results show that the combination of Cu/Al_2O_3 catalyst and ethanol was critical for the growth of bamboo-like MWCNTs. The possible factors causing the formation of bamboo-like structures were also discussed.

Introduction

As typical one-dimensional nanomaterials, carbon nanotubes (CNTs) have attracted wide research interests because of their excellent electrical, mechanical, and physico-chemical properties as well as their potential applications [1–5]. In recent years, following the extensive research of the preparation of CNTs, many novel shapes of CNTs were discovered, for example, bamboo-like [6–8], conical [9], Y shape [10], etc. Unlike conventional straight CNTs, bamboo-like CNTs consist of a series of separated hollow compartments. Owing to their unique structure, bamboo-like CNTs possess excellent electrical properties and could be potentially used in many fields [11, 12]. CNTs with bamboo-like structure have been prepared by a variety of methods such as arc discharge [13], pyrolysis of organometallic precursors [11], solventhermal synthesis [14], and chemical vapor deposition (CVD) [6–8]. However, in most above cases, a mixture of bamboo-like and conventional straight CNTs (or other morphologies of CNTs) was always obtained [13, 15]. Among these methods of preparation of bamboo-like CNTs, CVD possesses simple and low-cost features. Therefore, it would be necessary for developing a CVD growth of CNTs with dominant bamboo-like morphology in order to study the properties and applications of bamboo-like CNTs.

Generally, Fe, Co, and Ni are considered as the effective catalyst components in CVD growth of CNTs, while other metal elements are thought of as low activity components because of their poor carbon solubility or multiple carbide phases [16]. However, in recent years, non-iron group metal elements such as Au, Ag, Pt, Pd, Re, and Ru have shown catalytic active in CVD growth of CNTs [11, 12, 17–19]. It is worth to note that, study of the growth of CNTs over non-iron group catalyst is of great significance. It not only will promote further understanding of the growth mechanism of CNTs, but also may facilitate the research on novel morphologies of CNTs. Compared with the case of iron group catalysts, only few works have been reported for copper catalyzing synthesis of CNTs. For instance, CNTs have been synthesized on an alkali-element-modified Cu catalyst [20]. Synthesis of multiwalled carbon nanotubes (MWCNTs) has been achieved on Cu catalyst with a Lewis super acidic site [21]. Highly activated Cu nanoparticles can catalyze growth of single-walled carbon nanotubes (SWCNTs) [22].

B. Xue · R. Liu · Z.-D. Xu (✉)
Department of Chemistry, Zhejiang University, Hangzhou 310027, China
e-mail: materchemst@126.com

W.-Z. Huang · Y.-F. Zheng
Research Center of Analysis and Measurement, Zhejiang University of Technology, Hangzhou 310014, China

However, as far as we know, there is no report on synthesis of MWCNTs with bamboo-like morphology over non-modified Cu catalyst.

In this work, a facile and efficient CVD process has been developed to synthesize dominant bamboo-like MWCNTs. The reaction was carried out over the non-modified Cu/Al_2O_3 catalyst using ethanol as carbon source under atmospheric pressure between 750 and 850 °C. The morphology, microstructure, and graphitization degree of the products were characterized.

Experimental details

As a catalyst support, Al_2O_3 was synthesized according on a similar procedure in the literature [23]. Typically, 1.6 g NH_4HCO_3 and 37.5 g $Al(NO_3)_3 \cdot 9H_2O$ were dissolved in 200 mL distilled water, followed by slow addition of aqueous ammonia (10 wt%) under stirring until pH of solution reached about 8. The products were filtered, dried at 120 °C for 12 h, then calcined at 550 °C for 4 h, and finally ground to obtain Al_2O_3 powder.

Cu/Al_2O_3 catalysts were obtained through impregnating as-prepared Al_2O_3 with copper(II) acetate monohydrate. The solid residue was dried at 80 °C for 12 h and calcined at 550 °C for 4 h. The Cu/Al_2O_3 catalysts were obtained with copper contents of about 5.0 wt%.

Growth of MWCNTs was carried out in a quartz tube (4.5 cm of inner diameter and 110 cm in length) with a tube furnace as the reactor. A total of 50 mg Cu/Al_2O_3 catalyst was put into a quartz boat located at the center of the reactor. The reactor was heated up to the designed temperature at a heating rate of 10 °C/min in N_2 (99.999%) atmosphere. N_2 gas saturated by ethanol was then induced into the quartz tube at a flow rate of 400 mL/min. After reacting for 120 min, the reactor was cooled down in N_2. In order to remove the disturbance of catalyst support Al_2O_3, the products were dipped in hydrofluoric acid (40%) for 24 h, and then dried at room temperature.

The products were characterized by transmission electron microscopy (TEM, JEM 200CX), X-ray diffraction (XRD, Thermo ARL X'TRA), Raman spectroscopy (Almega Dispersive Raman, $\lambda_{exc} = 532$ nm), field emission scanning electron microscopy (FESEM, SIRION-100), and high-resolution transmission electron microscopy (HRTEM, JEM-2010) equipped with the selected area electron diffraction (SAED) device.

Results and discussion

Figure 1 shows the typical TEM images of MWCNTs grown over Cu/Al_2O_3 catalyst at 700, 750, 800, and 850 °C, respectively. The diameter distributions of MWCNTs were 20–50, 40–90, 30–80, and 50–90 nm, and the percentages of bamboo-like MWCNTs were 40, 85, 95, and 90% for 700, 750, 800, and 850 °C, respectively. Obviously, except for Fig. 1a (at 700 °C), other TEM

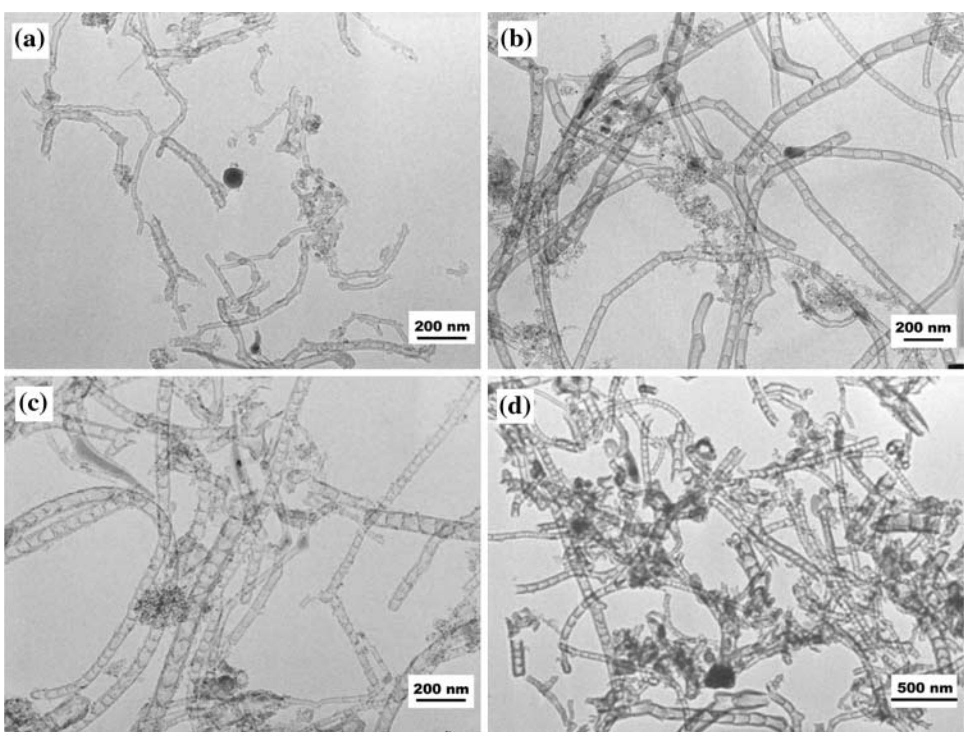

Fig. 1 TEM images of bamboo-like MWCNTs grown over Cu/Al_2O_3 catalyst at **a** 700 °C, **b** 750 °C, **c** 800 °C, and **d** 850 °C

images show that the products were dominated with bamboo-like MWCNTs. It is also clearly shown that the hollow compartments of bamboo-like tubes have a uniform size. However, the bamboo-like morphology of CNTs produced at 700 °C was not completely grown. It indicates that the reaction temperature plays a key role in the formation of the bamboo-like structures and the favorite reaction temperature exceeds over 700 °C. There is no significant difference of bamboo-like morphology among MWCNTs in Fig. 1b–d and this indicates that the growth of dominant bamboo-like MWCNTs can be achieved between 750 and 850 °C.

In order to investigate the crystal structure of the Cu catalyst particles and the bamboo-like MWCNTs, fresh catalyst and final products were characterized by XRD. As shown in Fig. 2A, XRD pattern of fresh Cu/Al_2O_3 catalyst reveals that the diffraction peaks of Al_2O_3 exist, but there are no obvious diffraction peaks of Cu species (e.g., CuO or Cu_2O, etc.). The possible reason for this case is that Cu species are not in crystal state or the amount of Cu catalyst particle is below the detection limits. In Fig. 2B–E, except for the case of 700 °C, the products synthesized at other three temperatures have a diffraction peak at about $2\theta = 26°$ and the peak is corresponding to graphite carbon (002) reflection. The intensity of this peak increased with the increase of the growth temperature. It indicates that growth of bamboo-like MWCNTs over Cu/Al_2O_3 catalyst takes place at temperature higher than 750 °C (including 750 °C). This result is consistent with TEM observations in Fig. 1. For all products, two clear diffraction peaks appear at $2\theta = 43.2°$ and 50.4° which can be indexed as (111) and (200) reflections associated with the face-centered cubic (fcc) phase of Cu, and the diffraction peaks of Al_2O_3 disappear due to corrosive effect of hydrofluoric acid. XRD results suggest that non-crystal state or dispersive Cu species have been converted to highly crystalline fcc metal phase during the growth of bamboo-like MWCNTs. The change of Cu species in the existence state may be related to the production mechanism of bamboo-like MWCNTs.

Raman spectroscopy is a very effective technique for characterizing the quality of CNTs [24, 25]. Figure 3 shows the Raman spectra of MWCNTs grown over Cu/Al_2O_3 catalyst at 750, 800, and 850 °C, respectively. In the spectra, the peaks at 1347 cm^{-1} correspond to polycrystalline graphite and disordered carbon (D-band). There are also other peaks located at 1580, 1589, and 1601 cm^{-1} for MWCNTs prepared at 750, 800, and 850 °C, respectively. The peak located at around 1590 cm^{-1} is related with one of the E_{2g} mode of single crystalline graphite (G-band). The intensity ratios of D-band to G-band (I_D/I_G) are 1.75,

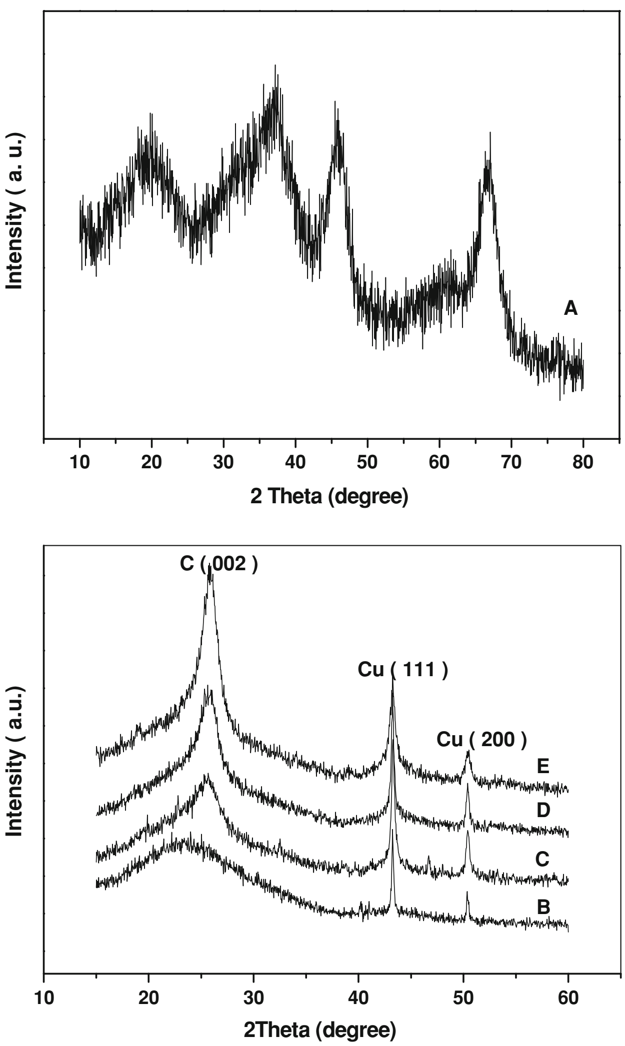

Fig. 2 (A) XRD pattern of fresh Cu/Al_2O_3 catalyst and XRD patterns of bamboo-like MWCNTs grown over Cu/Al_2O_3 catalyst at (B) 700 °C, (C) 750 °C, (D) 800 °C, and (E) 850 °C

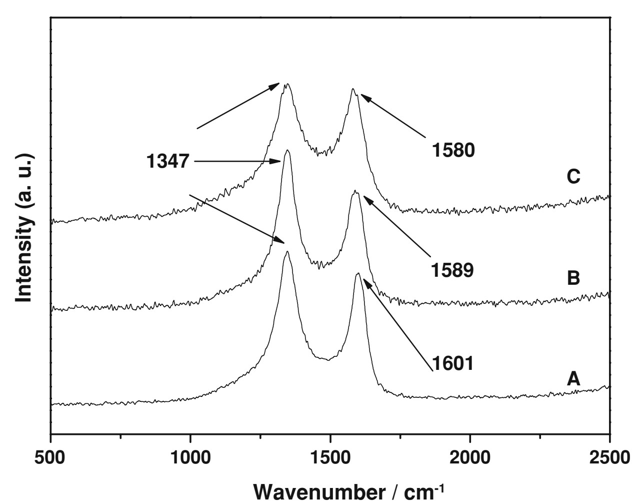

Fig. 3 Raman spectra of bamboo-like MWCNTs grown over Cu/Al_2O_3 catalyst at (A) 750 °C, (B) 800 °C, and (C) 850 °C. Arrows show the accurate position of peaks

1.48, and 1.72 for MWCNTs prepared at 750, 800, and 850 °C, respectively. In general, bamboo-like MWCNTs have stronger D-band and larger I_D/I_G values due to more defects, curves, and dislocations of graphitic sheets [11], and that is consistent with the aforementioned data. However, the I_D/I_G value of the MWCNTs grown at 800 °C is smaller than that grown at the other two temperatures. It indicates that the MWCNTs grown at 800 °C have relatively high quality with fewer defects.

For further research, the morphologies and microstructures of bamboo-like MWCNTs grown at 800 °C over Cu/Al_2O_3 catalyst were carefully investigated by FESEM, TEM, HRTEM, and SAED. The results are shown in Figs. 4 and 5. In FESEM image (Fig. 4a), CNTs with smooth outer wall are observed while branched nanotubes can also be found partially. Figure 4b shows that bamboo-like and branched structures appear simultaneously. Bamboo-like MWCNTs consist of nested-cone compartments with nearly equal size (about 30–50 nm of inner diameter and 40–60 nm in length) and are accompanied with Y-junction bifurcations. Moreover, bamboo-like MWCNTs with an open end can be seen, as marked with arrow in Fig. 4b, indicating that some tubes might be broken in the preparation of TEM sample under ultrasound treatment. In previous papers [10, 14], such branched structures could be observed occasionally, and often associated with bamboo-like structures. It is suggested that the formation of unique Y-junction bifurcation structures may be related to changing growth environment of graphite layers at a different location on the catalyst particle surface [26]. Different morphologies of catalyst particles are displayed in Fig. 4c, d. The two typical morphologies are plug-like and needle-like. Plug-like catalyst particles are commonly observed in the end of conventional MWCNTs. However, as far as we know, needle-like morphology of catalyst particles is relatively rare [20]. Such unique morphology reflects the quasi-liquid characteristic of Cu catalyst particles in the growth of bamboo-like MWCNTs, because Cu nanoparticles would exist in a quasi-liquid form due to their lowering melting point (about 850 °C) [27]. Moreover, it should be noted that encapsulated residual catalyst metallic impurities in CNTs have certain toxicity for organism. This remains major obstacles in the utilization of CNTs in many areas of science and technology. Many reports focused on removal of metallic impurities in CNTs [28–31]. Therefore, the toxicity and removal of residual Cu catalyst particles in bamboo-like MWCNTs need to be further investigated.

The microstructures of bamboo-like MWCNTs grown at 800 °C over Cu/Al_2O_3 catalyst are shown in Fig. 5. The HRTEM image in Fig. 5a reveals that the as-prepared CNTs have outer walls containing 9–12 nm thick graphite layers while the graphite layers of inner compartment only have a thickness of about 4 nm. Moreover, graphite layers of the wall on both sides of CNTs are arrayed in herringbone shapes with an angle (α) of about 35° between the tube axis and the graphite layer planes. Such a phenomenon is prevalent in bamboo-like MWCNTs [7] and may be

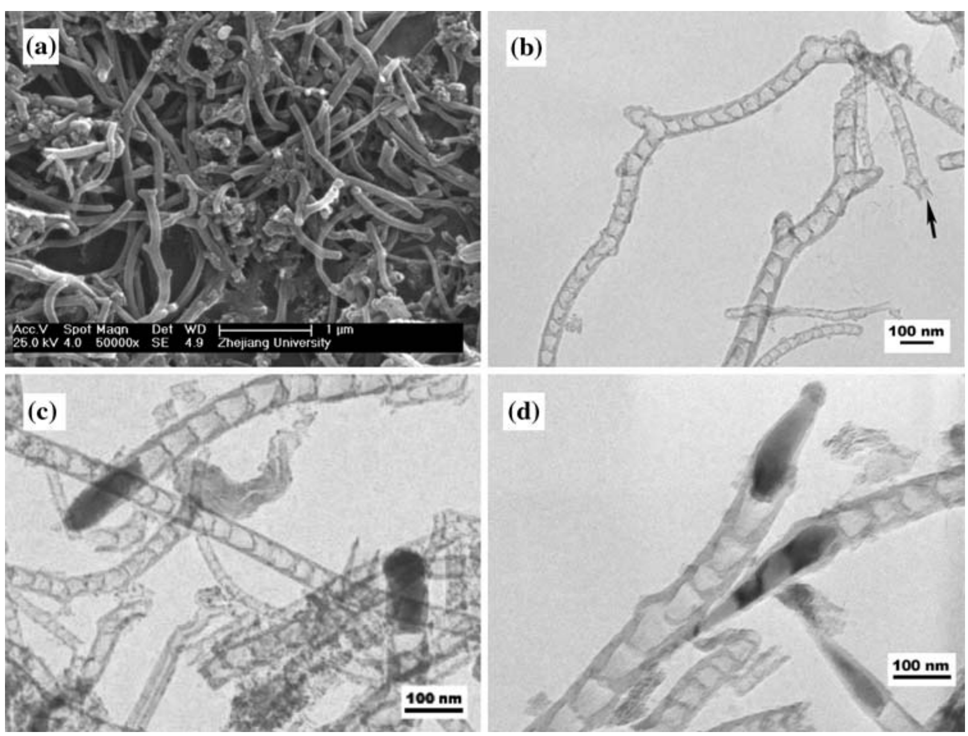

Fig. 4 Representative morphologies of bamboo-like MWCNTs grown at 800 °C over Cu/Al_2O_3 catalyst: **a** typical FESEM image, **b** TEM image of Y-junction bifurcation structures, **c** TEM image of plug-like catalyst particles, and **d** TEM image of needle-like catalyst particles

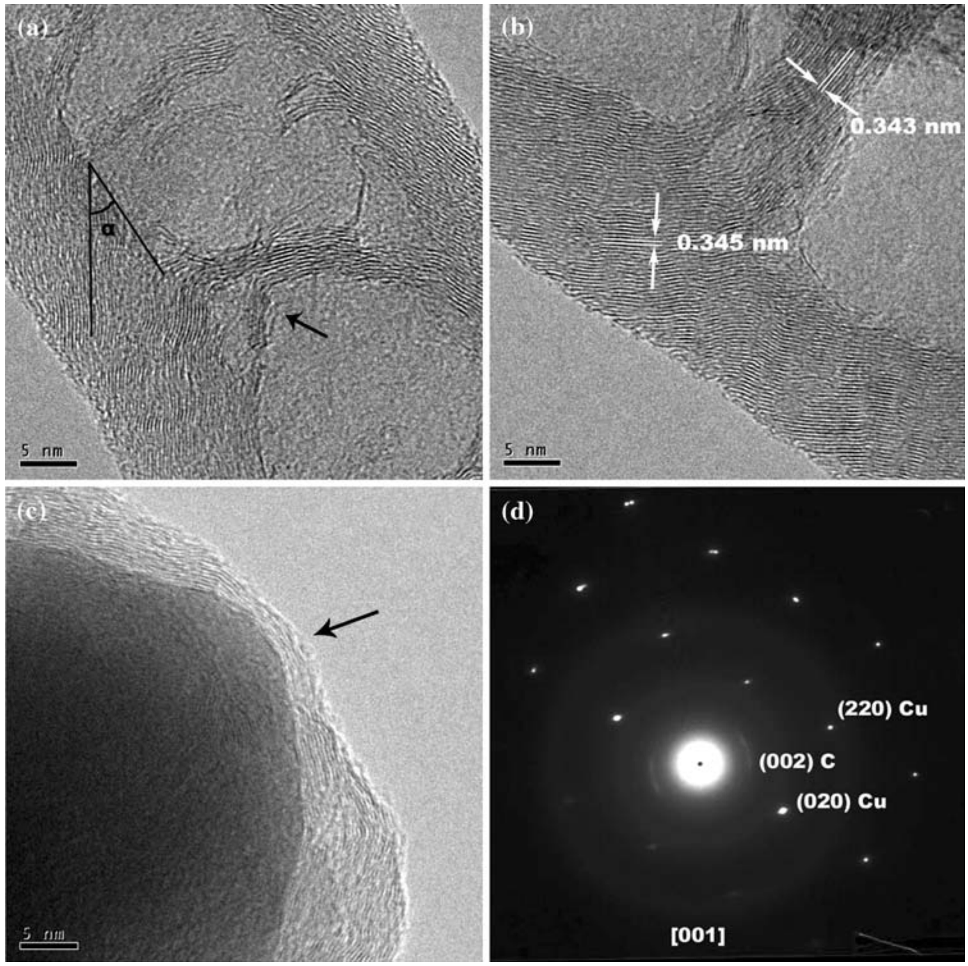

Fig. 5 Microstructures of bamboo-like MWCNTs grown at 800 °C over Cu/Al_2O_3 catalyst: **a**, **b**, and **c** HRTEM images, **d** SAED pattern of a catalyst part

correlated with the growth modes. The results in Fig. 5b show that the spacing of graphite layers is about 0.345 and 0.343 nm for outer walls and inner compartment, respectively. These values are close to that (0.34 nm) of conventional MWCNTs, which correspond to the (002) plane lattice parameter of graphite layers. Some disorder of graphite layers in outer walls and inner compartment can be found in Fig. 5a, b, indicating that the bamboo-like MWCNTs possess more defects, curves, and dislocations on graphitic sheets. Moreover, it is worth to note that the thickness of compartment graphite layers is not uniform and much thinner than that of sidewalls, as marked with arrow in Fig. 5a. Interestingly, non-uniformity of graphite layers covering the surface of the encapsulated catalyst particle was found, as marked with arrow in Fig. 5c. This widespread phenomenon in our results suggests that the formation of inner compartment graphite layers in bamboo-like MWCNTs may be related to the uneven diffusion and deposition of carbon on catalyst particle. Furthermore, through SAED analysis in Fig. 5d, the conversion of Cu catalyst particles into single crystal with fcc phase has been confirmed. The result is in good agreement with foregoing XRD patterns in Fig. 2B–E.

Based on the previous reports about Cu catalyzing CNTs [20, 21], the assistant role of Lewis acid/base or nano-size activation effect was necessary for catalysts. However, the Cu/Al_2O_3 catalyst in our case has not been specially modified in acid–base properties and particle size. This implies that the combination of Cu/Al_2O_3 catalyst and ethanol as carbon source is critical in the growth of bamboo-like MWCNTs. For comparison, catalytic growth of carbon materials has been examined using methanol or acetylene as the carbon source at 800 °C over Cu/Al_2O_3 catalyst, but no MWCNTs were obtained, as shown in Fig. 6. This greatly supports our hypothesis. It is well known that Cu-based catalysts are popularly employed in the ethanol dehydrogenation reactions [32]. Moreover, ethanol has higher reactivity than other usual carbon source such as CO and methane, because of lower activation energy for ethanol decomposition [33]. This may be a possible reason for effects of ethanol in our case. It might be attributed to the more effective activation of ethanol over Cu/Al_2O_3 catalyst than methanol and acetylene in the same reaction conditions.

To the best of our knowledge, growth mechanism of bamboo-like MWCNTs is not entirely clear so far. Many

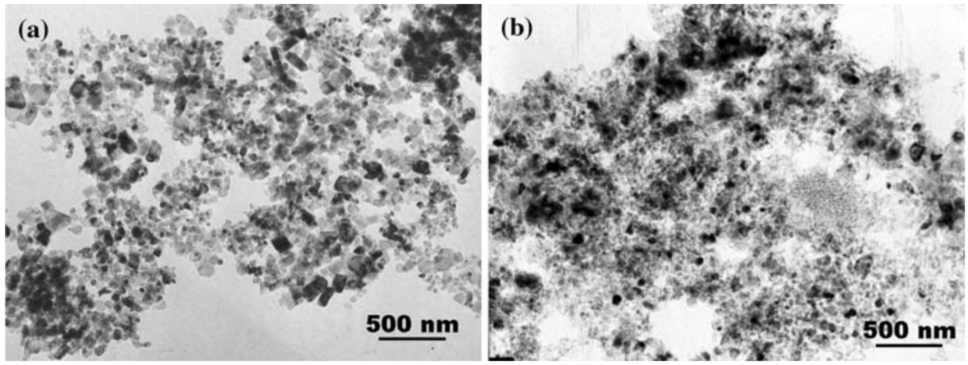

Fig. 6 The products grown at 800 °C over Cu/Al_2O_3 catalyst using other carbon sources: **a** methanol and **b** acetylene

authors proposed the possible mechanism on the basis of their experimental results. Smith et al. [34] put forward that bamboo morphology in carbon nanotubes may be the result of subtle changes in the growth conditions near the seed metal. Wu et al. [9] pointed out that formed conical nanoparticles lead to growth of bamboo-like CNTs. Zhao et al. [35] suggested that the difference between the carbon surface and bulk diffusion in the catalyst causes the periodic compartment structures in the bamboo-shaped CNTs. In our study, it can be seen that catalyst particles were encapsulated on closed-end bamboo-like MWCNTs in Figs. 4c, d and 5c. These observations suggest that the growth mode of bamboo-like MWCNTs over Cu/Al_2O_3 catalyst may be consistent with the tip-growth mode in the classical VLS (vapor-liquid-solid) mechanism [36]. Moreover, Cu catalyst nanoparticles tend to form needle-like (conical) morphology owing to lower melting point. Also, non-uniformity of diffusion and deposition of carbon on Cu catalyst particle possibly exists according to the VLS mechanism. These factors may be the causes of bamboo-like MWCNTs. Of course, the exact growth modes of bamboo-like MWCNTs over Cu/Al_2O_3 catalyst need to be further investigated.

Conclusions

The growth of bamboo-like MWCNTs over Cu/Al_2O_3 catalyst by CVD under atmospheric pressure using ethanol as the carbon source has been demonstrated. The obtained MWCNTs showed dominant bamboo-like morphology. The morphologies, graphitization degree, and microstructures of the products were systematically studied. The results show that the combination of Cu/Al_2O_3 catalyst and ethanol was critical for the growth of bamboo-like MWCNTs. The possible factors causing the formation of bamboo-like structures were also discussed. This study provides a facile and effective method to synthesize dominant bamboo-like MWCNTs. The majority bamboo-like structure obviously differs from the past mixture situation of bamboo-like and conventional straight CNTs. It should be beneficial for further investigating the unique structures, properties, and applications of bamboo-like MWCNTs.

Acknowledgements This study was supported by the Opening Foundation of Zhejing Provincial Top Key Discipline, the Zhejiang Provincial Natural Science Foundation of China (Y405131), Scientific Research Foundation for Returned Oversea Chinese Scholar of State Education Ministry (G50621), and Scientific Research Foundation for the Doctoral Degree Program of Higher Education of China (20070335156).

References

1. Iijima S (1991) Nature 354:56
2. Dai HJ (2002) Acc Chem Res 35:1035
3. Tasis D, Tagmatarchis N, Bianco A, Prato M (2006) Chem Rev 106:1105
4. Li X, Chen WX, Zhao J, Xing W, Xu ZD (2005) Carbon 43:2168
5. Chen WX, Tu JP, Wang LY, Gan HY, Xu ZD, Zhang XB (2003) Carbon 41:215
6. Chen JL, Li YD, Ma YM, Qin YN, Chang L (2001) Carbon 39:1467
7. Zhang XX, Li ZQ, Wen GH, Fung KK, Chen JL, Li YD (2001) Chem Phys Lett 333:509
8. He CN, Zhao NQ, Shi CS, Du XW, Li JJ (2007) Mater Lett 61:4940
9. Wu XC, Tao YR, Lu YN, Dong L, Hu Z (2006) Diam Relat Mater 15:164
10. Deng D, Lee JY (2007) Chem Mater 19:4198
11. Shanmugam S, Gedanken A (2006) J Phys Chem B 110:2037
12. Shanmugam S, Gedanken A (2006) Electrochem Commun 8:1099
13. Saito Y, Yoshikawa T (1993) J Cryst Growth 134:154
14. Du JM, Kang DJ (2006) Mater Res Bull 41:1785
15. Wu J, Hamaoui BE, Li J, Zhi L, Kolb U, Mullen K (2005) Small 1:210
16. Deck CP, Vecchio K (2006) Carbon 44:267
17. Takagi D, Homma Y, Hibino H, Suzuki S, Kobayashi Y (2006) Nano Lett 6:2642
18. Ritschel M, Leonhardt A, Elefant D, Oswald S, Bulchner B (2007) J Phys Chem C 111:8414
19. Reyhani A, Mortazavi SZ, Akhavan O, Moshfegh AZ, Lahooti Sh (2007) Appl Surf Sci 253:8458
20. Tao XY, Zhang XB, Cheng JP, Liu F, Li Y, Van Tendeloo G (2006) Nanotechnology 17:224
21. Lin JH, Chen CS, Ma HL, Hsu CY, Chen HW (2007) Carbon 45:223
22. Zhou WW, Han ZY, Wang JY, Zhang Y, Jin Z, Sun X, Zhang YW, Yan CH, Li Y (2006) Nano Lett 6:2987

23. Zhang SJ, Li LD, Xue B, Chen JX, Guan NJ, Zhang FX (2006) React Kinet Catal Lett 89:81
24. Dervishi E, Li Z, Biris AR, Lupu D, Trigwell S, Biris AS (2007) Chem Mater 19:179
25. Mahanandia P, Vishwakarma PN, Nanda KK, Prasad V, Barai K, Mondal AK, Sarangi S, Dey GK, Subramanyam SV (2008) Solid State Commun 145:143
26. Su LF, Wang JN, Yu F, Sheng ZM (2005) Chem Vap Deposition 11:351
27. Schaper AK, Hou H, Greiner A, Schneider R, Phillipp F (2004) Appl Phys A 78:73
28. Kolodiazhnyi T, Pumera M (2008) Small 4:1476
29. Flahaut E, Durrieu MC, Remy-Zolghadri M, Bareille R, Baquey CH (2006) J Mater Sci 41:2411. doi:10.1007/s10853-006-7069-7
30. Wen CY, Huang CC, Cheng HZ, Lu HY (2008) J Mater Sci 43:123. doi:10.1007/s10853-007-1779-3
31. Rocco AM, da Silva CA, Macedo MIF, Maestro LF, Herbst MH, Solorzano G, Xavier AL (2008) J Mater Sci 43:557. doi:10.1007/s10853-007-2122-8
32. Chang FW, Kuo WY, Lee KC (2003) Appl Catal A 246:253
33. Huang LM, Cui XD, White B, O′Brien SP (2004) J Phys Chem B 108:16451
34. Smith DK, Lee DC, Korgel BA (2006) Chem Mater 18:3356
35. Zhao NQ, He CN, Ding J, Zou TC, Qiao ZJ, Shi CS, Du XW, Li JJ, Li YD (2007) J Alloys Compd 428:79
36. Dupuis A-C (2005) Prog Mater Sci 50:929